Macroporous Hydrogels Upregulate Osteogenic Signal Expression and Promote Bone Regeneration

Martha W. Betz,[†] Andrew B. Yeatts,[†] William J. Richbourg,[†] John F. Caccamese,[‡] Domenick P. Coletti,[‡] Erin E. Falco,[§] and John P. Fisher*[,†,‡,§]

Fischell Department of Bioengineering and Department of Chemical and Biomolecular Engineering, University of Maryland, College Park, Maryland 20742, and Department of Oral and Maxillofacial Surgery, University of Maryland Dental School, Baltimore Maryland 21201

Received August 14, 2009; Revised Manuscript Received February 19, 2010

The objective of this work was to investigate the effects of macroporous hydrogel architecture on the osteogenic signal expression and differentiation of human mesenchymal stem cells (hMSCs). In particular, we have proposed a tissue engineering approach for orbital bone repair based on a cyclic acetal biomaterial formed from 5-ethyl-5-(hydroxymethyl)-β,β-dimethyl-1,3-dioxane-2-ethanol diacrylate (EHD) and poly(ethylene glycol) diacrylate (PEGDA). The EHD monomer and PEGDA polymer may be fabricated into macroporous EH-PEG hydrogels by radical polymerization and subsequent porogen leaching, a novel technique for hydrophilic gels. We hypothesized that EH-PEG hydrogel macroporosity facilitates intercellular signaling among hMSCs. To investigate this phenomenon, hMSCs were loaded into EH-PEG hydrogels with varying pore size and porosity. The viability of hMSCs, the expression of bone morphogenetic protein-2 (BMP-2), BMP receptor type 1A, and BMP receptor type 2 by hMSCs, and the differentiation of hMSCs were then assessed. Results demonstrate that macroporous EH-PEG hydrogels support hMSCs and that this macroporous environment promotes a dramatic increase in BMP-2 expression by hMSCs. This upregulation of BMP-2 expression is associated by a more rapid hMSC differentiation, as measured by alkaline phosphatase expression. Altering hMSC interactions with the EH-PEG hydrogel surface, by the addition of fibronectin, did not appear to augment BMP-2 expression. We therefore speculate that EH-PEG hydrogel macroporosity facilitates autocrine and paracrine signaling by localizing endogenously expressed factors within the hydrogel's pores and thus promotes hMSC osteoblastic differentiation and bone regeneration.

Introduction

There is a critical need to develop better clinical strategies for the treatment of craniofacial bone tissue defects. Orbital floor injuries, in particular, are a devastating form of trauma accounting for approximately 60−70% of all orbital fractures and are most commonly caused by assault and traffic accidents.[1−3] Orbital bone fractures heal poorly because only small bone fragments and few bony edges are present to conduct bone formation and restore orbital volume. Therefore, the normal response to orbital fractures, in contrast with many other bone fractures, is not sufficient for proper healing. Alternatively, improper treatment may lead to unsatisfactory facial aesthetics, enophthalmos (sunken eye), and diplopia.[4,5] Given that the orbital floor is a thin structure, ∼0.5 mm, it is an excellent model for in vitro tissue engineering because the nutritional limitations associated with larger tissue engineered constructs are minimized.[6,7]

Current alloplastic implants that are available for clinical use in orbital floor repair include Teflon, silicone, Gelfilm, Medpor (high-density polypropylene), and titanium.[2,6,8] However, an ideal biomaterial with favorable cellular interactions, mechanical strength, degradation, and degradation products, is not available. To this end, our laboratory has developed a class of biomaterials based on a cyclic acetal unit. Cyclic acetals may be preferred for tissue engineering applications because they hydrolytically degrade to form diol and carbonyl primary degradation products, which should not affect the local acidity of the implant or phenotypic function of a delivered cell population. A cyclic acetal biomaterial in the form of a rigid plastic may be fabricated from the radical polymerization of the monomer 5-ethyl-5-(hydroxymethyl)-β,β-dimethyl-1,3-dioxane-2-ethanol diacrylate (EHD).[9] The hydrophilic polymer poly(ethylene glycol) (PEG) may be incorporated to create a cyclic acetal-based hydrogel that could be used to deliver cell populations and growth factors.[10] Previous work has demonstrated that EH-PEG hydrogels support long-term viability of encapsulated bone marrow stromal cells.[11] In addition, EH-PEG hydrogels were able to deliver bone morphogenetic protein-2 to an orbital floor defect and support new bone growth, indicating that EH-PEG hydrogels are a viable craniofacial bone tissue engineering system.[12] However, this work also demonstrated that bulk hydrogels often prevent significant cell and tissue invasion because of their tight polymer network.

To improve bone regeneration and tissue integration, a tissue engineering scaffold should mimic bone morphology, structure, and function.[13] Scaffold porosity should also allow vascularization as well as enhanced tissue integration.[14] There is a number of studies in the literature reporting minimum pore sizes for osteogenesis. Interconnected pores with diameters >50 μm have been shown to be favorable to new bone formation, whereas the minimum pore size for osteoconduction is thought to be 80−100 μm.[15−18] Lastly, for the scaffold to support new vasculature, previous studies have shown that the minimum pore

* To whom correspondence should be addressed. Address: Fischell Department of Bioengineering, University of Maryland, 3238 Jeong H. Kim Engineering Building (no. 225), College Park, Maryland 20742. Tel: 301 405 7475. Fax: 301 405 0523. E-mail: jpfisher@umd.edu. Web: http://www.terpconnect.umd.edu/∼jpfisher.

[†] Fischell Department of Bioengineering, University of Maryland.

[‡] Department of Chemical and Biomolecular Engineering, University of Maryland.

[§] University of Maryland Dental School.

10.1021/bm100061z
Published on Web 03/26/2010

size is 45−100 μm; however, scaffolds with pore sizes of 100−150 μm resulted in a richer blood supply.[15,19] Whereas work has been conducted on scaffolds with micropores (<10 μm) and macropores (up to 500 μm), these results generally indicate that a minimum pore size of 100 μm is necessary for osteoconduction and vascularization.[13,20,21] On the basis of these works, we proposed to develop macroporous EH-PEG hydrogels with pore sizes ranging from 100 to 250 μm.

Transport phenomena concepts indicate that macroporosity within EH-PEG hydrogels may also facilitate both molecular diffusion and cell migration. We therefore hypothesized that this environment may facilitate autocrine and paracrine signaling. However, high porosity scaffolds can be associated with poor mechanical integrity. Engineering these properties to allow for appropriate diffusion and mechanical strength are important challenges in the construction of bone tissue engineering scaffolds. In this work and to the best of our knowledge for the first time, the effect of scaffold architecture in macroporous EH-PEG hydrogels on osteogenic signal expression of hMSCs was investigated. Specifically, the objectives of this work were to (1) investigate the effects of EH-PEG hydrogel scaffold architecture (porosity and pore size) on the expression of the osteogenic signal bone morphogenetic protein-2 (BMP-2) as well as its receptors, (2) examine the effect of adhesion through incorporating the extracellular matrix protein fibronectin in EH-PEG hydrogels on osteogenic signal expression, and (3) investigate the strength of EH-PEG scaffolds with varying pore size and porosity.

Methods

Materials. Ammonium persulfate (APS), *N*,*N*,*N*′,*N*′-tetramethylethylenediamine (TEMED), PEGDA $M_n \approx 700$, benzoyl peroxide, *N*,*N*-dimethyl-*p*-toludine, ascorbic acid Na-β-glyerophosphate, dexamethasone, and trizol were purchased from Sigma (St. Louis, MO) Human fibronectin and Quantikine BMP-2 immunoassay ELISA kit were purchased from R&D Systems (Minneapolis, MN). The DNeasy tissue kit and RNeasy mini plus kit were purchased from Qiagen (Valencia, CA). The live/dead assay and Quant-iT PicoGreen kit were ordered from Molecular Probes (Carlsbad, CA). High-glucose DMEM, MSC-qualified fetal bovine serum (FBS), penicillin-streptomycin antibiotics, L-glutamine, and nonessential amino acids were obtained from Invitrogen (Carlsbad, CA). The M-per mammalian protein extraction reagent was ordered from Pierce (Rockford, IL). The high capacity cDNA archive kit and TaqMan gene expression assays were purchased from Applied Biosystems (Foster City, CA). Stainless steel sieves were purchased from Fisher Scientific (Pittsburgh, PA) in the appropriate sizes.

5-Ethyl-5-(hydroxymethyl)-β,β-dimethyl-1,3-dioxane-2-ethanol Diacrylate Synthesis. EHD was synthesized on the basis of the previous protocols described by Kaihara et al.; other sources provide additional background on the EHD chemistry.[9−11,22] In brief, potassium carbonate (18.9 g, 0.25 equiv) was added to isobutyraldehyde (50 mL, 1 equiv) and formaldehyde (37% aqueous solution, 40.8 mL, 1 equiv) and the solution was stirred at 0 °C overnight. The product 3-hydroxy-2,2-dimethylpropinaldehyde (HDP) was extracted three times with chloroform and then washed with water and brine. The chloroform layers were combined and dried with sodium sulfate and the solvent was evaporated under reduced pressure to obtain solid HDP. HDP (32.9 g, 1 equiv) and trimethylolpropane (86.6 g, 2 equiv) were dissolved in 1 M hydrochloric acid (200 mL) and stirred for 2 h at 80 °C. The solution was then neutralized with sodium hydroxide, and the product 5-ethyl-5-(hydroxymethyl)-β,β-dimethyl-1,3-dioxane-2-ethanol (HEHD) was extracted three times with chloroform and washed with water and brine. The chloroform layers were combined and again dried with sodium sulfate and evaporated under reduced pressure to obtain solid HEHD. The HEHD was purified using an ethyl ether wash to remove undesired byproducts and was dried under reduced pressure. HEHD (31.3 g, 1 equiv) was dissolved in chloroform, and trimethylamine (65.4 mL, 3 equiv) and hydroquinone (0.034 g, 0.002 equiv) were added. Acryloyl chloride (38.1 mL, 3 equiv) was added dropwise as the reaction was stirred at 0 °C for 2 h. The insoluble salts were removed through filtration and the product, EHD, was extracted three times with chloroform and washed with water and brine. The chloroform layers were combined and dried with sodium sulfate and evaporated under reduced pressure. The EHD was further purified by silica gel column chromatography using a chloroform/ethanol (10:1 v/v) as the eluent. The fractions that contained EHD were determined by thin layer chromatography and NMR.

Hydrogel Formation. Porous EH-PEG constructs were cross-linked using APS and TEMED at 15 mM using a sodium chloride leaching technique. A saturated salt solution was used as the water component of the gel to slow the sodium chloride crystals from dissolving into the gel solution. The constructs were prepared using EHD and PEGDA $M_n \approx 700$ at 1:10 molar EHD to PEGDA with 30 wt % initial monomer components. Sieves were used to sort sodium chloride to approximately 100 or 250 μm sizes. Hydrogel pore size was determined by porogen size, and hydrogel mass porosity was determined by the porogen content. Four macroporous hydrogel groups were therefore examined: 250 μm porogen size/75% mass porosity, 250 μm porogen size/70% mass porosity, 100 μm porogen size/70% mass porosity, and 100 μm porogen size/65% mass porosity. These parameters were based on previous developments of scaffolds for bone tissue engineering applications.[23−26] Macroporous hydrogels were cut to 8 mm diameter with a cork borer, and sodium chloride was leached out over 2 days in water. Gels were sterilized in 70% ethanol, washed in PBS, and presoaked in control media plus FBS before cell loading.

We have previously developed an imaging technique based on optical coherence tomography to describe the pore characteristics of the macroporous EH-PEG hydrogels.[27] This work demonstrated that the hydrogels fabricated with 100 μm porogen resulted in pores ~80 μm in size (81.8 ± 14.1 and 80.4 ± 5.6 μm for the 65 and 70% mass porosity hydrogels, respectively), and those fabricated with 250 μm porogen resulted in pores ~130 μm in size (133.8 ± 23.2 and 132.7 ± 26.3 μm for the 70 and 75% mass porosity hydrogels, respectively).

Human Mesenchymal Stem Cell Culture. hMSCs, from a single donor, were purchased from Lonza and cultured according the manufacturer's specifications and as described in the literature.[28] Prior to the study, the hMSCs were cultured in control media composed of high glucose DMEM with 4 mM L-glutamine, 0.1 mM nonessential amino acids, 1% penicillin/streptomycin (v/v), and 10% MSC qualified FBS. During the study, the osteogenic groups were supplemented with 100 nM dexamethasone, 10 mM Na-β-glyerophosphate, and 0.2 mM ascorbic acid. hMSCs (passage <5) were added to sterile, presoaked hydrogels in a concentrated cell solution (0.3 to 2.0 × 10^5 cells/scaffold). The cells were allowed to attach for 4 h before filling the well with media. The media was changed every two days throughout the study. All data describing hMSC and differentiated cell phenotype were normalized by cell number. We do not present cell proliferation data because of the difficulty associated with retrieval of the entire cell population from the macroporous hydrogel. Two basic control groups were included in the examination of hMSC and differentiated cell phenotype. A normal control examined a monolayer of hMSCs grown on tissue culture polystyrene dishes and grown in control media. An osteogenic control examined a monolayer of hMSCs grown on tissue culture polystyrene dishes and grown in osteogenic media. A final control group consisted of hMSCs grown on EH-PEG hydrogel disks and grown in osteogenic media.

Fibronectin Loading. The hydrogels were loaded with fibronectin in a sterile environment before use. Specifically, surface liquid was removed from hydrogels and allowed to dry in a sterile environment for 1 h. Then, a concentrated solution of fibronectin was added and

allowed to absorb for ~1 h for final concentrations of 0.5, 2.5, and 10 μg fibronectin/gel. Then, the hMSCs were added as previously described.

Protein Assays. Total protein was extracted using the M-per mammalian protein extraction reagent as previously described.[11] A *p*-nitrophenyl phosphate liquid substrate system (pNPP) was used to analyze intracellular ALP concentrations. The absorbance was read using a M5 SpectraMax plate reader at 405 nm. Data were normalized to the DNA. Bone morphogenetic protein-2 protein levels from culture media were measured using a quantikine ELISA kit (R&D systems) and a M5 SpectraMax platereader. At each time point, the media was removed and centrifuged to remove particulates and then frozen until analysis. DNA was isolated from all samples to normalize the assay using the DNeasy Tissue kit (Qiagen). DNA was then quantified using the Quant-iT PicoGreen Kit (Molecular Probes) and read with excitation/emission of 480/520 nm.

Viability. Cell-laden hydrogels were cultured and analyzed throughout the study using the live/dead assay, as previously described.[11] At each time point, the cell−hydrogel constructs were soaked in PBS for 1.5 h to remove FBS from the hydrogel that can interact with the live/dead reagents. The constructs were incubated with the live/dead reagents (2.5 μm ethidium homodimer-1 and 2.5 μm calcein AM) at room temperature for 30 min. Micrographs were then taken using a fluorescence microscope equipped with a digital camera.

Gene Expression. RNA was isolated from cells in monolayer using the RNeasy Mini Plus Kit following standard protocols. The RNA was isolated from the hMSCs in EH-PEG hydrogels using trizol and purified using the RNeasy mini kit following standard protocols. The isolated total RNA was reverse transcribed using the high capacity cDNA archive kit. The expressions of bone morphogenetic protein-2, bone morphogenetic protein receptors 1A and 2 (BMP-R1A and BMP-R2), and osteocalcin were then investigated by quantitative real-time polymerase chain reaction (qrt-PCR) on an ABI Prism 7000 sequence detector (Applied Biosystems) with GAPDH as an endogenous control. TaqMan gene expression assays were used for all genes, and the sequences are proprietary.

Trilayer Formation and Testing. Trilayer scaffolds were constructed from two layers of porous EH-PEG bound to a central layer of porous EH, allowing the central EH layer to provide mechanical support to the EH-PEG hydrogels. The EH-PEG layers were cross-linked using 40 mM APS and TEMED. The EH layer was cross-linked using 7 wt % benzoyl peroxide and 8 μL of *N*,*N*-dimethyl-*p*-toludine per gram of EHD in acetone. The three layers were adhered by placing each on top of one another during cross-linking, allowing covalent bonding to occur across the layer interfaces. Trilayers were created with varying porosity and pore size for the EH layer, whereas for all conditions, the EH-PEG layer was held constant at 75 wt %. The two control groups were constructed from three layers of porous EH-PEG at each of the two pore sizes, lacking the central EH layer. Following polymerization, the scaffolds were soaked in acetone for 15 min. Sodium chloride was then leached out over 2 days in water. Flexural properties were then examined using a three-point bend test based on ASTM D 7264 standard test method for flexural properties of polymer matrix composite material. An INSTRON 5565 mechanical tester was employed, and Bluehill software was used to record load data until breaking. The preload was set at 0.01 N, and the extension rate was set at the standard 1 mm/min. Samples were prepared at a thickness of 4.00 mm (1.33 mm per layer), and a support span-to-thickness ratio at eight was used for testing. Flexural strength was calculated as $\sigma_{fs} = (3F_fL)/(2bd^2)$, where F_f is the load at fracture, L is the distance between support points, and b and d are the width and height of the specimen, respectively.[29]

Statistical Analysis. All samples were completed in triplicate ($n = 3$). Data from all studies were analyzed first using ANOVA single factor analysis and then Tukey's multiple comparison test to demonstrate differences between groups ($p \leq 0.05$). All results are reported as mean ± standard deviation. Please note that only pertinent statistical relationships are noted in the Figures.

Results

Investigation of Scaffold Architecture and Osteogenic Signal Expression. Because creating macroporous hydrogels through porogen leaching is not an established technique, we first developed a simple method for their fabrication. Here a hydrogel solution is saturated with salt; then, additional salt porogen is added to the solution. After polymerization and leaching in water, macroporous hydrogels are obtained. With these materials, we next endeavored to examine the effect of macroporous hydrogel architecture on hMSC phenotype and particularly their expression of osteogenic signals.

To this end, hMSCs were loaded into EH-PEG hydrogels with pore size/mass porosities of 250 μm/75%, 250 μm/70%, 100 μm/70%, and 100 μm/65%, and then analyzed for viability using the live/dead assay (Figure 1). After one day of culture, the cell populations appear viable in all groups independent of pore size and porosity. Cell viability was maintained throughout the 12 day study. It should be noted that during the study, whereas they were viable, the hMSCs did not demonstrate a high degree of spreading common with hMSC culture.

Bone morphogenetic protein-2 levels were then measured at the protein level by ELISA (Figure 2). Results indicate similar levels for all groups at day 1. However, by day 4, the hMSCs in EH-PEG hydrogels show significantly higher BMP-2 protein levels as compared with the controls ($p \leq 0.05$). These elevated levels are increased at day 8 and maintained throughout the study, where at day 12, hMSCs within EH-PEG hydrogels show BMP-2 levels ~40 times higher than hMSCs in monolayer controls. BMP-2 mRNA expression shows significantly elevated levels in all groups over the controls by day 1 and throughout the study, independent of pore size or porosity ($p \leq 0.05$, Figure 3a). At day 12, hMSCs in the 250 μm EH-PEG gels had BMP-2 mRNA fold changes of 67 and 64 for 75 and 70% mass porosity hydrogels, respectively, and in the 100 μm EH-PEG gels, a fold change of 26 and 90 for 70 and 65% mass porosity hydrogels, respectively, over the monolayer control. An additional control of hMSCs cultured in monolayer on EH-PEG hydrogel disks did not reveal the significant upregulation observed in the macroporous hydrogel environment (Figure 3b). Further analysis showed that this increase in BMP-2 mRNA expression correlated with an increase in BMP mRNA receptor expression (Figure 3c,d). The increase in receptor expression was again independent of scaffold architecture; however, the increase was not to the same magnitude as the BMP-2 mRNA increase because all groups demonstrated a fold change of ~2 at day 12.

Alkaline phosphatase, an early marker for osteoblastic differentiation, was analyzed on days 1, 4, 8, and 12 (Figure 4). Control groups were cultured in monolayer for all studies, and results indicate moderate changes in ALP expression from day 1 to day 4 for all groups. However, the hMSCs in the 100 μm EH-PEG hydrogels show significantly higher ALP expression at day 8, demonstrating a large increase from day 4 ($p \leq 0.05$). This represents a faster rate of ALP expression when compared with the ALP expression by hMSCs in the 250 μm EH-PEG gels and the osteogenic control. From day 8 to day 12, the hMSCs in the 100 μm EH-PEG hydrogels were associated with decreasing ALP expression levels, whereas the hMSCs in the 250 μm EH-PEG gels and the osteogenic control saw increased ALP levels. Osteocalcin expression was also analyzed; however, only low levels were detected, indicating that the hMSCs were

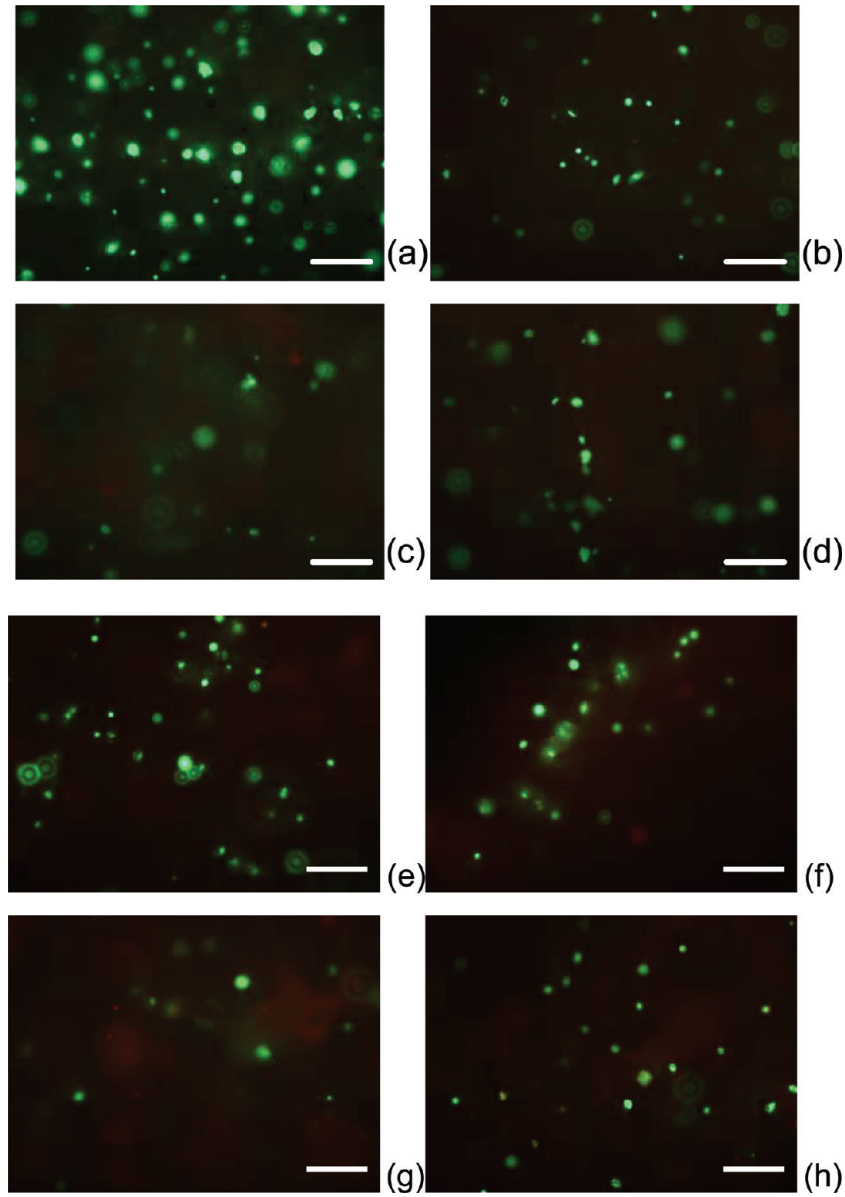

Figure 1. Viability of hMSCs in EH-PEG hydrogels. (a−d) After 1 day of culture and (e−h) after 12 days of culture, the majority of the hMSCs appear viable. Macroporous EH-PEG hydrogel with a (a,e) 100 μm porogen size/65% mass porosity, (b,f) 100 μm porogen size/70% mass porosity, (c,g) 250 μm porogen size/70% mass porosity, or (d,h) 250 μm porogen size/75% mass porosity. Scale bar denotes 250 μm.

not expressing the late-stage differentiation marker during this 12 day study.

Investigation of Cell Adhesion and Osteogenic Signal Expression. We next aimed to discriminate between the effects of scaffold architecture, previously described, and the effects of cell−scaffold adhesion on BMP-2 expression. We chose to examine this question using the EH-PEG hydrogels with 100 μm pore size and 65% mass porosity because of their apparent high BMP-2 expression and quick ALP expression. These hydrogel scaffolds were then prepared with the addition of fibronectin at concentrations of 0.5, 2.5, and 10.0 μg/gel. The viability of hMSCs in EH-PEG hydrogels with fibronectin was assessed throughout the study. For the duration of the investigation, the majority of the hMSCs appeared to be viable (Figure 5). In addition, and as expected, the hMSCs within EH-PEG hydrogels with higher concentrations of fibronectin demonstrated increased cell spreading. Whereas BMP-2 mRNA expression showed significantly elevated levels in all groups over the controls throughout the study ($p \leq 0.05$), the addition of fibronectin did not significantly alter BMP-2 expression. At days 4 and 8, hMSCs in EH-PEG gels with the highest concentrations of fibronectin demonstrated the highest expression of BMP-2 mRNA. Specifically, at day 8, hMSCs cultured in the 10.0 μg fibronectin/gel EH-PEG gels showed a fold change of 60 over the control. Further analysis showed that the increase in BMP-2 expression correlated with an increase in BMP receptor expression (Figures 6b,c), as demonstrated by significantly increased levels of BMP-R1A and BMP-R2 mRNA ($p \leq 0.05$). The increase in receptor mRNA levels was largely independent of fibronectin concentration. As shown in the previous section, the increase in receptor mRNA expression was not to the same magnitude as the BMP-2 mRNA increase, where the BMP-R1A increase was approximately 2-fold and the BMP-R2 increase was approximately 1.5-fold at day 12.

Investigation of Scaffold Architecture and Mechanical Strength. Macroporosity is known to reduce mechanical integrity. Therefore, whereas the inclusion of macroporosity into EH-PEG hydrogels may facilitate osteogenic signal expression, the resulting scaffold may also be too weak for clinical application. We therefore endeavored to fabricate multilayered scaffolds that would be

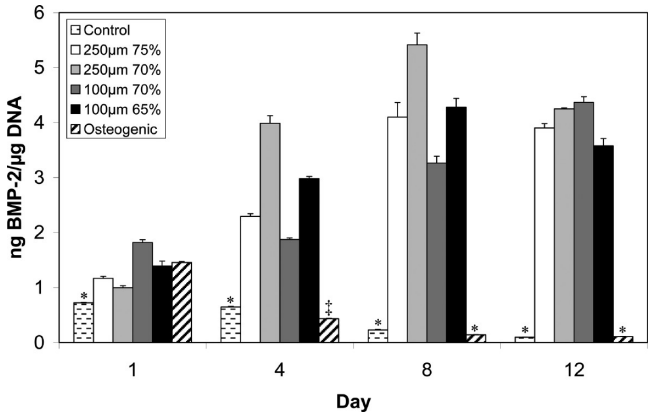

Figure 2. BMP-2 protein expression by hMSCs cultured in monolayer (control media or osteogenic media) or within macroporous EH-PEG hydrogels of varying pore size (100 or 250 μm) and porogen content (65, 70, or 75%). BMP-2 protein levels were measured by ELISA and normalized by DNA after 1, 4, 8, and 12 days. The results indicate similar levels for all groups at day 1; however, by day 4, the hMSCs in EH-PEG hydrogels show significantly higher levels as compared with the controls. These elevated levels are maintained throughout the study. The symbols (‡, *) denote statistical significance within that time point.

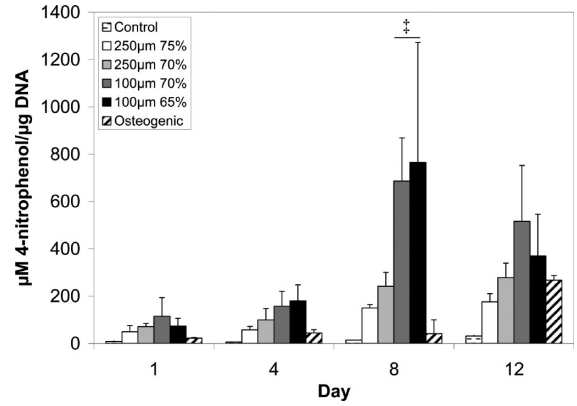

Figure 4. Alkaline phosphatase expression, normalized by DNA, by hMSCs cultured in monolayer (control media or osteogenic media) or within macroporous EH-PEG hydrogels of varying pore size (100 or 250 μm) and porogen content (65, 70, or 75%) after 1, 4, 8, and 12 days. The results indicate moderate changes from day 1 to day 4 for all groups. The hMSCs in the 100 μm EH-PEG gels showed a significant increase in expression from day 4 with a peak a day 8 demonstrating a faster rate of expression as compared to the osteogenic control. The symbol (‡) denotes statistical significance within that time point.

relevant to the repair of orbital floor fractures. Trilayer scaffolds were constructed from two layers of porous EH-PEG bound to a central layer of porous EH, allowing the central EH layer to provide mechanical support to the EH-PEG hydrogels (Figure 7). These trilayer scaffolds were created with varying porosity and pore size to determine their effects on mechanical strength. Results indicate

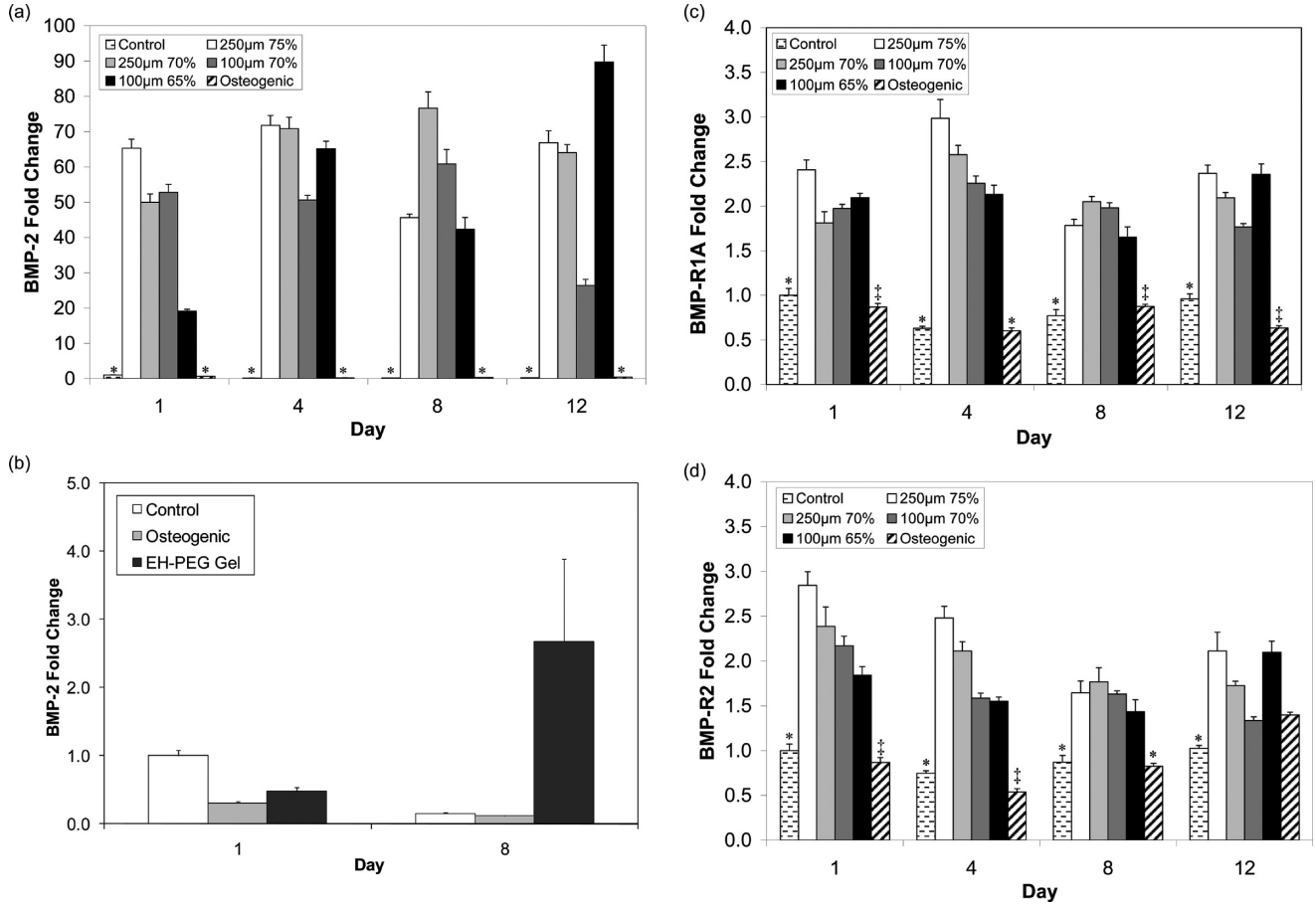

Figure 3. (a,b)BMP-2, (c) BMP-R1A, and (d) BMP-R2 mRNA expression by hMSCs cultured in monolayer (TCPS and control media, TCPS and osteogenic media, or EH-PEG and osteogenic media) or within macroporous EH-PEG hydrogels of varying pore size (100 or 250 μm) and porogen content (65, 70, or 75%). BMP-2 expression by hMSCs cultured in macroporous EH-PEG hydrogels shows significantly elevated levels over all controls throughout the study independent of pore size and porosity. (b,c) The increase in BMP-2 correlated with a significant increase in receptor expression. The elevated levels of BMP receptor expression are maintained throughout the study and are independent of pore size and porosity. The symbols (‡, *) denote statistical significance within that time point.

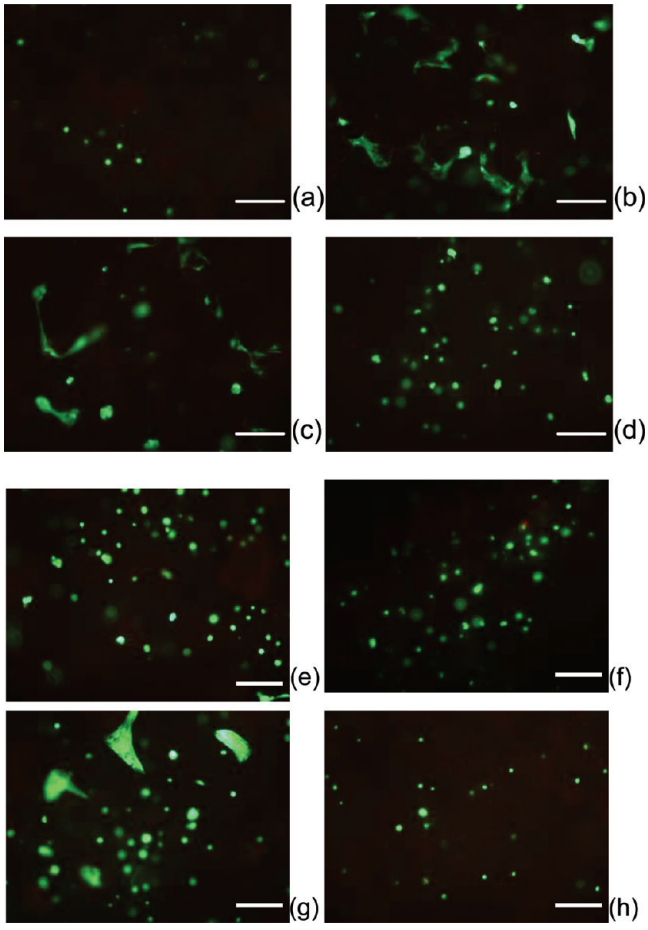

Figure 5. Viability of hMSCs when cultured within EH-PEG hydrogels (100 μm pore size and 65% mass porosity) with increasing concentrations of fibronectin ((a,e) 0.5 μg fibronectin per gel, (b,f) 2.5 μg fibronectin per gel, (c,g) 10.0 μg fibronectin per gel, and (d,h) 0 fibronectin per gel) and (a−d) after 4 days or (e−h) 8 days of culture. Higher concentrations of fibronectin demonstrate cell spreading. Scale bar denotes 250 μm.

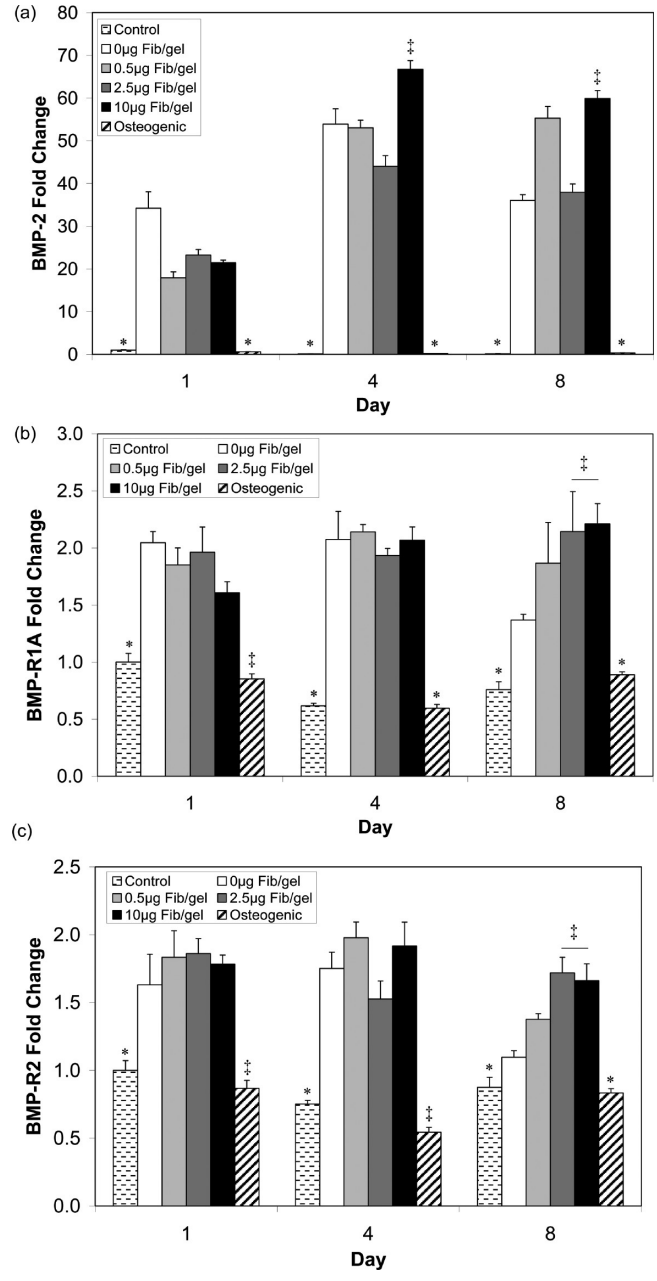

Figure 6. (a) BMP-2, (b) BMP-R1A, and (c) BMP-R2 mRNA expression by hMSCs cultured in monolayer (TCPS and control media, or TCPS and osteogenic media) or within EH-PEG hydrogels (100 μm pore size and 65% mass porosity) with increasing concentrations of fibronectin (0, 0.5, 2.5, or 10.0 μg fibronectin per gel). BMP-2 expression by hMSCs cultured in macroporous EH-PEG hydrogels shows significantly elevated levels over all controls throughout the study, with a slight increase from day 1 to day 4. (b,c) This increase in BMP-2 expression is correlated with a significant increase in receptor expression. The elevated levels of BMP receptor expression by hMSCs cultured in macroporous EH-PEG hydrogels is maintained throughout the study and appears to have a slight dependence on fibronectin concentration, where the higher concentrations demonstrate higher receptor expression. The symbols (‡, *) denote statistical significance within that time point.

that the scaffolds demonstrated increasing strength with decreasing porosity when comparing scaffolds with the same pore size. (See Figure 8.) The trilayer scaffolds at 250 μm did show a slight increase in strength over the EH-PEG control. However, the trilayer scaffolds at 100 μm showed significantly higher strength when compared with the control and to the 250 μm scaffolds ($p \leq 0.05$).

Discussion

We demonstrate here that macroporous EH-PEG hydrogels upregulate hMSC's endogenous expression of BMP-2 and therefore facilitate hMSC osteoblastic differentiation. Because hydrogel architecture is a key feature of this work, we began by developing an elegant means for fabricating macroporous hydrogels. A number of techniques have been utilized to create porous scaffolds for tissue engineering applications, and porogen leaching has been implemented frequently with non-water-soluble polymers. Macroporous water-swollen hydrogels, however, have been more commonly fabricated by freeze-drying, stereolithography, or gas-foaming.[30−36] We have shown that an EHD monomer and PEGDA polymer may be fabricated into a macroporous EH-PEG hydrogel by radical polymerization and porogen leaching. Here a saturated salt was used as the water component of the gel to slow the dissolution of the salt porogen, thus creating a macroporous hydrogel. We should note that hydrogels are typically utilized for cell encapsulation.[11] Using the porogen leaching technique described here, cells are not embedded within the bulk of hydrogels but rather are seeded onto the surface of the pores throughout the macroporous hydrogel scaffold. Therefore, the cell−material interface is largely 2D rather than the 3D interface observed in encapsulation.

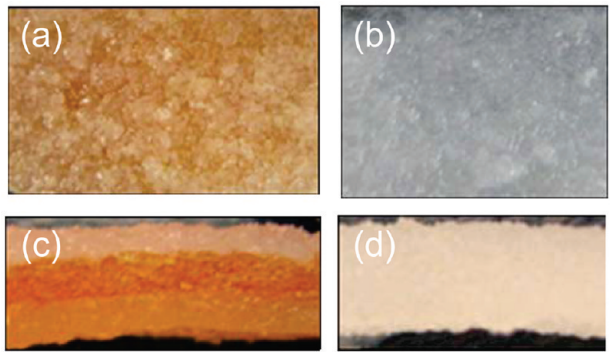

Figure 7. Scaffolds for mechanical testing. (a,c) Trilayer scaffolds and (b,d) control EH-PEG gels. (a,b) Top view of scaffold and (c,d) side view demonstrates layers.

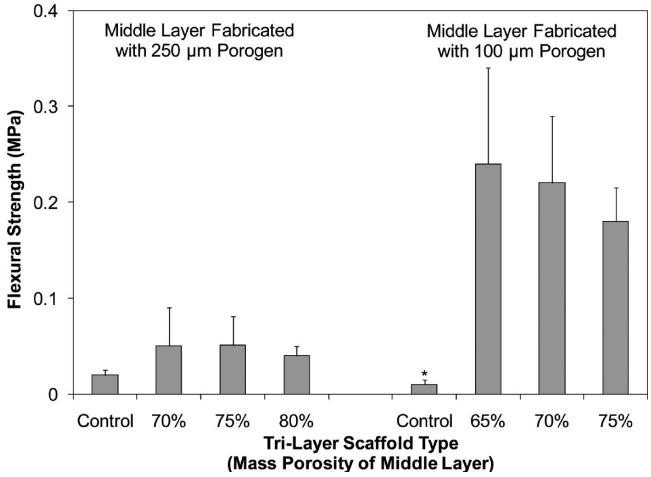

Figure 8. Flexural strength of trilayer scaffolds consisting of a porous EH layer sandwiched between two macroporous EH-PEG hydrogels. Parameters refer to the pore size (100 or 250 μm) and porogen content (65, 70, 75, or 80%) of the middle EH layer; the EH-PEG layer was held constant at 75% porogen content. Control samples consisted of a trilayer of EH-PEG hydrogels. Results indicate increasing strength with decreasing porogen content within the same pore size. The trilayer scaffolds fabricated with 100 μm porogen showed significantly higher strength when compared with the control trilayer hydrogels and with those scaffolds fabricated with 250 μm porogen. The symbol (*) denotes statistical significance within that pore size.

We next investigated the effect of varying macroporous hydrogel architecture on hMSC's endogenous expression of osteogenic signals and, in particular, their expression of BMP-2 and BMP-2 receptors. BMP-2 is known to increase mesenchymal stem cell proliferation and differentiation into osteoblasts.[37] In addition, BMP-2 has chemotactic effects on human osteoblasts.[38] BMP signaling has been shown to be involved in a number of functional osteoblast pathways including bone matrix proteins, osteogenic regulatory genes, BMP inhibitory factors, and osteogenic transcription factors.[39] BMP receptors also play a critical role in signaling. The two membrane-bound BMP receptors, type 1A and type 2, are both able to bind the soluble BMP-2.[40] It is thought that signal transduction requires the formation of a complex between the type IA and type II receptors before ligand binding, and binding initiates a signal cascade within the cell.[39−41]

To examine their osteogenic response, hMSCs were seeded on EH-PEG scaffolds with varying porosity and pore size, and then compared with cells cultured in monolayer. Initial work demonstrated that hMSC viability was maintained throughout the study (Figure 1); however, hMSCs do not appear as spread as in standard cultures. Results then demonstrated a dramatic increase in BMP-2 expression when hMSCs are cultured within the macroporous environment when compared with monolayer controls. Beginning 4 days after seeding, hMSCs demonstrated significantly higher levels of BMP-2 expression than those cultured in monolayer (Figures 2 and 3); control groups grown in monolayer on TCPS or EH-PEG disks showed similar trends (Figure 3b). This upregulation was dramatic, in the range of 50−70 fold for some groups. The existence of macroporous hydrogel architecture is thought to be the key parameter because significant differences were not noted among the pore size and porosity examined. We suggest that this macroporous environment facilitates autocrine and paracrine signaling by localizing endogenously expressed factors within the hydrogel's water filled pores. We believe that this is among the first observations of this effect. Furthermore, this phenomenon may become a powerful means for controlling stem cell differentiation. Previous studies have demonstrated the ability of substrate stiffness to impact the differentiation of hMSCs.[42] Specifically, after several weeks in culture, cells commit to a lineage specified by matrix elasticity. Whereas this may have an effect on the hMSCs in our macroporous EH-PEG hydrogel system because the osteogenic signal expression increased significantly at day 4, we suggest that the architectural effect we have observed is either an underlying or discrete phenomenon.

Alternatively, hMSCs grown within macroporous EH-EPG hydrogels showed only modest increases in the expression of BMP-2 receptor molecules, BMP-R1A and BMP-R2. We suggest that this result provides further support to our proposed relationship between hydrogel architecture and BMP-2 expression. First, because the same approach is used to quantify the expression of BMP-2 and the receptors BMP-R1A and BMP-R2, any assay bias toward hMSCs grown among the hydrogels should be similar. However, the upregulation observed in the case of BMP-2 is on the order of 50−70 fold, whereas that observed with the BMP-2 receptors is much less (two to three fold). Second, because BMP-2 is soluble and the receptors are membrane bound, the hypothesis that macroporous architecture promotes autocrine and paracrine signaling by localizing soluble factors within the hydrogel's pores is consistent with the dramatic upregulation of BMP-2 and modest change in BMP receptors.

hMSCs within EH-PEG hydrogels were then analyzed for alkaline phosphatase levels, an early osteogenic marker, to investigate if increased osteogenic signal expression enhances differentiation. Results again showed a quicker and enhanced osteogenic response, as measured by ALP expression, for those hMSCs grown within the macroporous EH-PEG hydrogels (Figure 4). We suggest that this difference in ALP levels, which did appear to be dependent on pore size and porosity, could reflect the presence of higher BMP-2 levels that were observed in these groups. We note that osteocalcin expression was also measured; however, only low levels were detected, revealing that the late osteogenic marker is not being expressed in the 12 days of this study.

Results from the previous studies indicate that the ideal EH-PEG architecture to use for hMSC culture was 100 μm pore size and 65% mass porosity. We then chose to add the extracellular matrix protein fibronectin to the EH-PEG hydrogels because fibronectin is known to aid in hMSC attachment.[43,44] This environment should be conducive to differentiation and therefore may enhance osteogenic cell signaling. Furthermore, this should allow us to contrast the effects of cell adhesion and modified scaffold architecture on osteogenic signal expression. Results showed that the majority of the hMSCs were viable

and proliferated on the surfaces of the fibronectin-modified macroporous EH-PEG hydrogels (Figure 5). Furthermore, and as expected, hMSCs cultured on surfaces with higher concentrations of fibronectin demonstrated enhanced cell spreading as compared EH-PEG hydrogels with no fibronectin. When compared with monolayer controls, hMSCs cultured in EH-PEG hydrogels exhibit increased osteogenic signaling, as shown by BMP-2 expression and BMP receptor expression, with no dependence on fibronectin concentration (Figure 6). However, when compared with the BMP-2 expression from hMSCs cultured without the addition of fibronectin (Figures 2 and 3), we concluded that upregulated BMP-2 expression is predominately due to macroporous architecture, rather than an increase in cell adhesion from the incorporation of fibronectin in EH-PEG hydrogels. Therefore, culturing hMSCs within a macroporous EH-PEG seems to have significantly contributed to the early osteogenic signal expression and, as a result, osteoblastic differentiation.

One concern with the proposed approach is the effect of the macroporous architecture on the mechanical strength on the construct. Hydrogels are, in general, mechanically weak, and the fabrication of macroporous hydrogels creates an even weaker constructs. We therefore considered the clinical application of this approach, in particular, the implantation of macroporous EH-PEG hydrogels as bone tissue engineering constructs for the orbital floor. To address this concern, we altered EH-PEG hydrogels by introducing a stiff, but still porous central layer to improve support. The resulting trilayer scaffolds were tested in a three-point bend test for flexural properties that simulate the physiological stresses in situ for orbital floors. The results indicate increasing strength with decreasing porosity, as expected. The 100 μm trilayer scaffolds showed significant improvement over the 100 μm EH-PEG hydrogel and over the 250 μm trilayer scaffolds. It is possible that the scaffolds with the larger pore sizes and higher porosities may have improved interconnectivity, which may cause their decreased strength. Whereas it is interesting to see the difference in strength between the scaffolds with varying architecture, it is important to determine if the construct will support the orbital contents. It is difficult to perform mechanical studies on the human orbital floor because it is composed of portions of three bones, and the anatomy is difficult to simulate in animal models. However, the literature has reported that the combined weight of the human orbital contents is approximately 42.97 ± 4.05 g.[45] From this data, we can estimate the orbital contents would apply $\sim$0.13 MPa, which can be supported by our 100 μm scaffolds but exceeds the strength of the 250 μm scaffolds. This analysis indicates that the 100 μm scaffolds are an appropriate construct for orbital floor repair, whereas the 250 μm scaffolds may be appropriate for other applications.

Conclusions

The objective of this work was to investigate the effects of macroporous hydrogel architecture upon hMSC osteogenic signal expression and differentiation. Results showed that culturing hMSCs within a macroporous hydrogel architecture significantly upregulates BMP-2 expression and that this upregulation promotes quick differentiation. We speculate that this phenomenon may be primarily due to the macroporous architecture's ability to facilitate autocrine and paracrine signaling by localizing endogenously expressed factors within the hydrogel's water-filled pores. Future studies are required to examine whether the biomaterial itself plays a significant role in promoting osteogenic signal expression. We suggest that the results of this work may provide an important means to direct stem cell differentiation beyond those previously described in the literature. Finally, the results of this study should have a significant impact on the development of biomaterials for stem cell therapies.

Acknowledgment. This work was supported by the National Science Foundation (CAREER Award to J.P.F., no. 0448684) and the State of Maryland, Maryland Stem Cell Research Fund.

References and Notes

(1) Eski, M.; Sahin, I.; Deveci, M.; Turegun, M.; Isik, S.; Sengezer, M. A retrospective analysis of 101 zygomatico-orbital fractures. *J. Craniofacial Surg.* **2006**, *17*, 1059–1064.
(2) Rinna, C.; Ungari, C.; Saltarel, A.; Cassoni, A.; Reale, G. Orbital floor restoration. *J. Craniofacial Surg.* **2005**, *16*, 968–972.
(3) Manolidis, S.; Weeks, B. H.; Kirby, M.; Scarlett, M.; Hollier, L. Classification and surgical management of orbital fractures: experience with 111 orbital reconstructions. *J. Craniofacial Surg.* **2002**, *13*, 726–737; discussion 738.
(4) Burnstine, M. A. Clinical recommendations for repair of orbital facial fractures. *Curr. Opin. Ophthalmol.* **2003**, *14*, 236–240.
(5) Ellis, E., III.; Tan, Y. Assessment of internal orbital reconstructions for pure blowout fractures: cranial bone grafts versus titanium mesh. *J. Oral Maxillofacial Surg.* **2003**, *61*, 442–453.
(6) Chang, E. W.; Manolidis, S. Orbital floor fracture management. *Facial Plast. Surg.* **2005**, *21*, 207–213.
(7) *Oral and Maxillofacial Surgery*; Fonseca, R., Ed.; Saunders: Philadelphia, PA, 2000; Vol. 3, pp 205−243.
(8) Donati, L.; Baruffaldi-Preis, F. W.; Di Leo, A.; Donati, V.; Cavallini, M.; Marazzi, M.; Falcone, L. Ten-year experience with craniofacial implants: clinical and experimental results. *Int. Surg.* **1997**, *82*, 325–331.
(9) Moreau, J. L.; Kesselman, D.; Fisher, J. P. Synthesis and properties of cyclic acetal biomaterials. *J. Biomed. Mater. Res., Part A* **2007**, *81*, 594–602.
(10) Kaihara, S.; Matsumura, S.; Fisher, J. P. Synthesis and characterization of cyclic acetal based degradable hydrogels. *Eur. J. Pharm. Biopharm.* **2008**, *68*, 67–73.
(11) Betz, M. W.; Modi, P. C.; Caccamese, J. F.; Coletti, D. P.; Sauk, J. J.; Fisher, J. P. Cyclic acetal hydrogel system for bone marrow stromal cell encapsulation and osteodifferentiation. *J. Biomed. Mater. Res., Part A* **2008**, *86*, 662–670.
(12) Betz, M. W.; Caccamese, J. F.; Coletti, D. P.; Sauk, J. J.; Fisher, J. P. Tissue response and orbital floor regeneration using cyclic acetal hydrogels. *J. Biomed. Mater. Res., Part A* **2009**, *90*, 819−829.
(13) Karageorgiou, V.; Kaplan, D. Porosity of 3D biomaterial scaffolds and osteogenesis. *Biomaterials* **2005**, *26*, 5474–5491.
(14) Story, B. J.; Wagner, W. R.; Gaisser, D. M.; Cook, S. D.; Rust-Dawicki, A. M. In vivo performance of a modified CSTi dental implant coating. *Int. J. Oral Maxillofacial Implants* **1998**, *13*, 749–757.
(15) Kong, L.; Ao, Q.; Wang, A.; Gong, K.; Wang, X.; Lu, G.; Gong, Y.; Zhao, N.; Zhang, X. Preparation and characterization of a multilayer biomimetic scaffold for bone tissue engineering. *J. Biomater. Appl.* **2007**, *22*, 223–239.
(16) Lu, J. X.; Flautre, B.; Anselme, K.; Hardouin, P.; Gallur, A.; Descamps, M.; Thierry, B. Role of interconnections in porous bioceramics on bone recolonization in vitro and in vivo. *J. Mater. Sci.: Mater. Med.* **1999**, *10*, 111–120.
(17) White, E.; Shors, E. C. Biomaterial aspects of Interpore-200 porous hydroxyapatite. *Dent. Clin. North Am.* **1986**, *30*, 49–67.
(18) Gauthier, O.; Bouler, J. M.; Aguado, E.; Pilet, P.; Daculsi, G. Macroporous biphasic calcium phosphate ceramics: influence of macropore diameter and macroporosity percentage on bone ingrowth. *Biomaterials* **1998**, *19*, 133–139.
(19) Hulbert, S. F.; Morrison, S. J.; Klawitter, J. J. Tissue reaction to three ceramics of porous and non-porous structures. *J. Biomed. Mater. Res.* **1972**, *6*, 347–374.
(20) Simon, J. L.; Roy, T. D.; Parsons, J. R.; Rekow, E. D.; Thompson, V. P.; Kemnitzer, J.; Ricci, J. L. Engineered cellular response to scaffold architecture in a rabbit trephine defect. *J. Biomed. Mater. Res., Part A* **2003**, *66*, 275–282.
(21) Yuan, H.; Kurashina, K.; de Bruijn, J. D.; Li, Y.; de Groot, K.; Zhang, X. A preliminary study on osteoinduction of two kinds of calcium phosphate ceramics. *Biomaterials* **1999**, *20*, 1799–1806.

(22) Kaihara, S.; Matsumura, S.; Fisher, J. P. Synthesis and properties of poly[poly(ethylene glycol)-*co*-cyclic acetal] based hydrogels. *Macromolecules* **2007**, *40*, 7625–7632.
(23) Fisher, J. P.; Holland, T. A.; Dean, D.; Engel, P. S.; Mikos, A. G. Synthesis and properties of photocross-linked poly(propylene fumarate) scaffolds. *J. Biomater. Sci., Polym. Ed.* **2001**, *12*, 673–687.
(24) Fisher, J. P.; Lalani, Z.; Bossano, C. M.; Brey, E. M.; Demian, N.; Johnston, C. M.; Dean, D.; Jansen, J. A.; Wong, M. E.; Mikos, A. G. Effect of biomaterial properties on bone healing in a rabbit tooth extraction socket model. *J. Biomed. Mater. Res., Part A* **2004**, *68*, 428–438.
(25) Fisher, J. P.; Vehof, J. W. M.; Dean, D.; van der Waerden, J. P. C. M.; Holland, T. A.; Mikos, A. G.; Jansen, J. A. Soft and hard tissue response to photocrosslinked poly(propylene fumarate) scaffolds in a rabbit model. *J. Biomed. Mater. Res.* **2002**, *59*, 547–556.
(26) Vehof, J. W.; Fisher, J. P.; Dean, D.; van der Waerden, J. P.; Spauwen, P. H.; Mikos, A. G.; Jansen, J. A. Bone formation in transforming growth factor beta-1-coated porous poly(propylene fumarate) scaffolds. *J. Biomed. Mater. Res.* **2002**, *60*, 241–251.
(27) Chen, C.; Betz, M.; Fisher, J.; Paek, A.; Jiang, J.; Ma, H.; Cable, A.; Chen, Y. Investigation of pore structure and cell distribution in EH-PEG hydrogel scaffolds using optical coherence tomography and fluorescence microscopy. *Proc. SPIE* **2010**, *7566*, 756603.
(28) Guo, L.; Kawazoe, N.; Hoshiba, T.; Tateishi, T.; Chen, G.; Zhang, X. Osteogenic differentiation of human mesenchymal stem cells on chargeable polymer-modified surfaces. *J. Biomed. Mater. Res., Part A* **2008**, *87*, 903–912.
(29) Callister, W. D. *Fundamentals of Materials Science and Engineering: An Integrated Approach*; 2nd ed.; John Wiley & Sons: Hoboken, NJ, 2005; p 1.
(30) Hsu, Y. Y.; Gresser, J. D.; Trantolo, D. J.; Lyons, C. M.; Gangadharam, P. R.; Wise, D. L. Effect of polymer foam morphology and density on kinetics of in vitro controlled release of isoniazid from compressed foam matrices. *J. Biomed. Mater. Res.* **1997**, *35*, 107–116.
(31) Mapili, G.; Lu, Y.; Chen, S.; Roy, K. Laser-layered microfabrication of spatially patterned functionalized tissue-engineering scaffolds. *J. Biomed. Mater. Res., Part B* **2005**, *75*, 414–424.
(32) Mathieu, L. M.; Mueller, T. L.; Bourban, P. E.; Pioletti, D. P.; Muller, R.; Manson, J. A. Architecture and properties of anisotropic polymer composite scaffolds for bone tissue engineering. *Biomaterials* **2006**, *27*, 905–916.
(33) Nam, Y. S.; Yoon, J. J.; Park, T. G. A novel fabrication method of macroporous biodegradable polymer scaffolds using gas foaming salt as a porogen additive. *J. Biomed. Mater. Res.* **2000**, *53*, 1–7.
(34) Sachlos, E.; Czernuszka, J. T. Making tissue engineering scaffolds work. Review: the application of solid freeform fabrication technology to the production of tissue engineering scaffolds. *Eur. Cells Mater.* **2003**, *5*, 29–39; discussion 39−40.
(35) Sheridan, M. H.; Shea, L. D.; Peters, M. C.; Mooney, D. J. Bioabsorbable polymer scaffolds for tissue engineering capable of sustained growth factor delivery. *J. Controlled Release* **2000**, *64*, 91–102.
(36) Whang, K.; Tsai, D. C.; Nam, E. K.; Aitken, M.; Sprague, S. M.; Patel, P. K.; Healy, K. E. Ectopic bone formation via rhBMP-2 delivery from porous bioabsorbable polymer scaffolds. *J. Biomed. Mater. Res.* **1998**, *42*, 491–499.
(37) Chu, T. M.; Warden, S. J.; Turner, C. H.; Stewart, R. L. Segmental bone regeneration using a load-bearing biodegradable carrier of bone morphogenetic protein-2. *Biomaterials* **2007**, *28*, 459–467.
(38) Lee, D. H.; Park, B. J.; Lee, M. S.; Lee, J. W.; Kim, J. K.; Yang, H. C.; Park, J. C. Chemotactic migration of human mesenchymal stem cells and MC3T3-E1 osteoblast-like cells induced by COS-7 cell line expressing rhBMP-7. *Tissue Eng.* **2006**, *12*, 1577–1586.
(39) Singhatanadgit, W.; Salih, V.; Olsen, I. RNA interference of the BMPR-IB gene blocks BMP-2-induced osteogenic gene expression in human bone cells. *Cell Biol. Int.* **2008**, *32*, 1362–1370.
(40) Wozney, J. M.; Rosen, V. Bone morphogenetic protein and bone morphogenetic protein gene family in bone formation and repair. *Clin. Orthop. Relat. Res.* **1998**, 26–37.
(41) Saito, N.; Murakami, N.; Takahashi, J.; Horiuchi, H.; Ota, H.; Kato, H.; Okada, T.; Nozaki, K.; Takaoka, K. Synthetic biodegradable polymers as drug delivery systems for bone morphogenetic proteins. *Adv. Drug Delivery Rev.* **2005**, *57*, 1037–1048.
(42) Engler, A. J.; Sen, S.; Sweeney, H. L.; Discher, D. E. Matrix elasticity directs stem cell lineage specification. *Cell* **2006**, *126*, 677–689.
(43) Ogura, N.; Kawada, M.; Chang, W. J.; Zhang, Q.; Lee, S. Y.; Kondoh, T.; Abiko, Y. Differentiation of the human mesenchymal stem cells derived from bone marrow and enhancement of cell attachment by fibronectin. *J. Oral Sci.* **2004**, *46*, 207–213.
(44) Salasznyk, R. M.; Williams, W. A.; Boskey, A.; Batorsky, A.; Plopper, G. E. Adhesion to vitronectin and collagen i promotes osteogenic differentiation of human mesenchymal stem cells. *J. Biomed. Biotechnol.* **2004**, *2004*, 24–34.
(45) Haug, R. H.; Nuveen, E.; Bredbenner, T. An evaluation of the support provided by common internal orbital reconstruction materials. *J. Oral Maxillofacial Surg.* **1999**, *57*, 564–570.

BM100061Z